Hyper-adhesion in desmosomes: its regulation in wound healing and possible relationship to cadherin crystal structure

David R. Garrod, Mohamed Y. Berika*, William F. Bardsley, David Holmes and Lydia Tabernero‡

Faculty of Life Sciences, Michael Smith Building, Oxford Road, University of Manchester, Manchester, M13 9PT, UK

*Present address: Department of Anatomy, Mansoura University, EL-Goumhouria Street, Mansoura, Egypt

‡Author for correspondence (e-mail: lydia.tabernero@manchester.ac.uk)

Accepted 9 September 2005
Journal of Cell Science 118, 5743-5754 Published by The Company of Biologists 2005
doi:10.1242/jcs.02700

Summary

The resistance of tissues to physical stress is dependent upon strong cell-cell adhesion in which desmosomes play a crucial role. We propose that desmosomes fulfil this function by adopting a more strongly adhesive state, hyper-adhesion, than other junctions. We show that the hyper-adhesive desmosomes in epidermis resist disruption by ethylene glycol bis(2-aminoethyl ether)-N,N,N′N′-tetraacetic acid (EGTA) and are thus independent of Ca^{2+}. We propose that Ca^{2+} independence is the normal condition for tissue desmosomes. Ca^{2+} independence is associated with an organised arrangement of the intercellular adhesive material exemplified by a dense midline. When epidermis is wounded, desmosomes in the wound-edge epithelium lose hyper-adhesiveness and become Ca^{2+} dependent, i.e. readily dissociated by EGTA. Ca^{2+}-dependent desmosomes lack a midline and show narrowing of the intercellular space. We suggest that this indicates a less-organised, weakly adhesive arrangement of the desmosomal cadherins, resembling classical cadherins in adherens junctions. Transition to Ca^{2+} dependence on wounding is accompanied by relocalisation of protein kinase C α to desmosomal plaques suggesting that an 'inside-out' transmembrane signal is responsible for changing desmosomal adhesiveness. We model hyper-adhesive desmosomes using the crystal packing observed for the ectodomain of C-cadherin and show how the regularity of this 3D array provides a possible explanation for Ca^{2+} independence.

Key words: Desmosome, Cadherin, Cell-cell adhesion, Wound healing, Protein kinase C

Introduction

Tissues such as cardiac muscle and epidermis are extremely resistant to shearing forces and physical stress. A vital contributing factor in stress resistance is strong intercellular adhesion mediated by cell-cell junctions. Among these is the desmosome, which is particularly abundant in tissues that are subject to stress. Analysis of human autoimmune and genetic disease, and targeted deletions of desmosomal genes in mice shows that abnormality of desmosomes leads to tissue disruption (reviewed by Chidgey, 2002; Garrod et al., 2002a; Garrod et al., 2002b; Getsios et al., 2004; Huber, 2003; McMillan and Shimizu, 2001; Payne et al., 2004; South, 2004).

Formation of intercellular adhesion appears to be initiated by adherens junctions and subsequently reinforced by desmosomes (Vasioukhin et al., 2000). The essential nature of desmosomal reinforcement is demonstrated by the loss of epidermal integrity, which occurs following conditional knockout of the desmosomal plaque protein desmoplakin from the epidermis (Vasioukhin et al., 2001). Thus it appears that desmosomes are of prime importance for maintaining tissue integrity. Apart from their abundance in tissues such as epidermis, which is well documented (Skerrow et al., 1989), no clear explanation for the ability of desmosomes to mediate strong intercellular adhesion has been advanced.

The principal adhesion molecules of both desmosomes and adherens junctions are cadherins, members of a large family of molecules that mediate Ca^{2+}-dependent cell-cell adhesion (Nollet et al., 2000). In adherens junctions these are classical cadherins such as E-cadherin, and in desmosomes they are the desmosomal cadherins, desmocollin and desmoglein. In accordance with the Ca^{2+}-dependent nature of these molecules, the formation and disruption of desmosomal adhesion have both been shown to be Ca^{2+} dependent (Hennings and Holbrook, 1983; Kartenbeck et al., 1982; Mattey and Garrod, 1986a; Mattey and Garrod, 1986b; Watt et al., 1984). However, Ca^{2+} dependence is only a temporary property of desmosomal adhesion; after initial desmosome assembly desmosomal adhesion becomes Ca^{2+} independent, which is resistant to disruption by reduction of extracellular Ca^{2+} concentration or Ca^{2+} chelation (Mattey and Garrod, 1986b; Watt et al., 1984).

Factors regulating the Ca^{2+} independence of desmosomes of Madin-Darby canine kidney (MDCK) cells in tissue culture have been investigated in some detail (Wallis et al., 2000). We showed that development of Ca^{2+} independence requires culture confluence. The desmosomes of cells maintained at subconfluent density do not progress beyond Ca^{2+} dependence. Moreover Ca^{2+}-independent desmosomes in confluent cell sheets revert to Ca^{2+} dependence when confluence is destroyed by wounding the cell sheet. Having been initiated at the wound edge, reversion to Ca^{2+} dependence is propagated through the

cell monolayer. Reversion to Ca^{2+} dependence occurs in the presence of cycloheximide and thus does not require protein synthesis. Rather, it appears to be regulated by protein kinase C (PKC) signalling because PKC activation promotes Ca^{2+} dependence and inhibition promotes Ca^{2+} independence. The change between Ca^{2+} dependence and Ca^{2+} independence caused by PKC activators and inhibitors is rapid (~15 minutes) and much less than the time thought to be required for desmosome assembly. Immunolocalisation and antisense depletion experiments showed that the PKCα isoform is involved in this regulation. The acquisition of Ca^{2+} independence is specific to desmosomes because adherens and tight junctions do not become Ca^{2+} independent (Wallis et al., 2000). We suggested that the modulation of desmosomal adhesion on disruption of epithelial confluence somehow facilitates downregulation of desmosomal adhesion and the promotion of cell migration in wound healing (Wallis et al., 2000). It was also shown that desmosomes in several mouse epithelial tissues are Ca^{2+} independent (Wallis et al., 2000). Previously desmosomes resistant to disruption by Ca^{2+} chelation have been reported in frog tissues (Borysenko and Revel, 1973).

Numerous studies have been carried out on the structural basis of adhesion by classical cadherins. A crystallographic study of the entire extracellular domain (EC1-EC5) of *Xenopus* C-cadherin showed that distal subdomains EC1-EC3 are involved in two main types of molecular interactions (Boggon et al., 2002). One is the 'strand dimer', which mediates trans interaction and is formed by the insertion of the side chain of a tryptophan residue (Trp2) near the N-terminus into a hydrophobic pocket of the EC1 subdomain of the partner molecule (Haussinger et al., 2004; Overduin et al., 1995; Shapiro et al., 1995). This trans interaction is interpreted as the adhesive interaction that occurs between two cell surfaces. The other type is a cis interaction. It involves interaction of the face of EC1 opposite Trp2 with the EC2-EC3 linker region of another molecule on the same cell surface. These cis and trans interactions generate a regular molecular 3D array, in which every EC1 domain forms both cis interactions with EC2-EC3 subdomains in parallel chains and trans interactions with the EC1 subdomain of anti-parallel chains (Boggon et al., 2002).

Desmocollins and desmogleins are cadherins whose extracellular domains have many features in common with classical cadherins. The interdomain Ca^{2+}-binding sites are fully conserved in the desmocollins and desmoglein 2, and largely conserved in the other desmogleins. Furthermore, there is evidence to suggest that the so-called cell adhesion recognition (CAR) site regions that form part of the hydrophobic pockets involved in classical cadherin strand dimer formation are also involved in adhesion by desmosomal cadherins (Runswick et al., 2001; Tselepis et al., 1998). It is thus reasonable to suppose that the molecular mechanism of adhesive interactions of desmosomal cadherins is similar to that of classical cadherins, although no structural studies of desmosomal cadherins have been published.

We set out to determine whether modulation of desmosomal Ca^{2+} dependence is an in vivo phenomenon, and have made some striking discoveries. Modulation of desmosomal adhesion, identical to that found in tissue culture, takes place on wounding epidermis. Changes in the structure of the desmosomal adhesive material that accompany modulation of desmosomal adhesion lead us to suggest a model for desmosomal Ca^{2+} independence based on the cadherin crystal structure. Furthermore we propose a novel concept, hyper-adhesion, which is unique to desmosomes and explains, for the first time, why they are so fundamentally important in maintaining the strength and integrity of vertebrate tissues.

Materials and Methods

Wounding studies

Two full-thickness wounds were made on the backs of male Balb-C mice aged 8-10 weeks according to published method (Tomlinson and Ferguson, 2003). After the times indicated in the text, figures and tables, the mice were killed and wound-edge material either frozen in liquid nitrogen for cryostat sectioning and immunofluorescence, or fixed and embedded for conventional transmission electron microscopy, or for ultra-thin cryosectioning and immuno-gold labelling. Control, unwounded skin was taken directly from freshly killed mice, without wounding.

Immunofluorescence

Frozen sections (15-20 μm thick) were collected on poly-L-lysine-coated slides and fixed for 5 minutes in acetone at room temperature. After rinsing with phosphate-buffered saline, they were incubated in 5% normal donkey serum and 1% bovine serum albumen for 10 minutes, before rinsing in PBS and incubating with monoclonal antibody to desmoplakin (11-5F) (see Parrish et al., 1987) and rabbit anti-PKCα (Sigma). Secondary antibodies were FITC-conjugated donkey anti-rabbit IgG and Rhodamine Red donkey anti-mouse IgG (Jackson ImmunoResearch Laboratories). Immunofluorescence was examined using a Zeiss LSM510 confocal microscope.

Electron microscopy

Transmission and immuno-gold EM were carried out as described (North et al., 1999). The primary anti-PKC antibody used for the latter was as for immunofluorescence. The secondary antibody was 10-nm-gold-conjugated goat anti-rabbit IgG (British Biocell International).

Analysis of PKCα distribution in the desmosomal plaque

Using electron micrographs printed at a total magnification of 46,000×, the distribution of PKCα with respect to the inner leaflet of the desmosomal plasma membrane was determined using two methods: manual measurement with a ruler and image analysis using the Scion Image Program (http://www.scioncorp.com). The same 48 desmosomes that were sectioned transversely were used for each determination. The desmosomes were labelled with the antibodies 11-5F to desmoplakin and anti-PKCα, using 20 nm gold particles for the former and 10 nm for the latter. The perpendicular distance of each gold particle from the inner leaflet of the plasma membrane was measured. Gold particles in the intercellular space were given a negative value. Measurements obtained manually were referred to as PKC1 (corresponding to PKCα) and DP1 (corresponding to desmoplakin), and those obtained by image analysis as PKC2 and DP2. The SIMFIT program (http://www.simfit.man.ac.uk), designed by Bill Bardsley (University of Manchester, UK) was used to analyse the data to determine whether (1) measurements obtained by the two techniques differ significantly; (2) the observations are scattered randomly or if there is evidence for significant clustering; and (3) the distributions can be quantified. For further details and results of this analysis, please refer to the authors.

Molecular modelling

The program SegMod (Levitt, 1992) was used to build a homology model for the sequences of Dsg2 and Dsc2 (Q14126, Q02487) using the C-cadherin ectodomain structure (1L3W.pdb) as a template. The initial models obtained were then refined according to the gradient minimisation routine in Xplor v3.8 (Brunger, 1987) to minimise van der Waals interactions. Following the minimisation, a 3D array of molecules was created based on the crystallographic cell and symmetry operations obtained in the 1L3W.pdb structure.

Results

Desmosomes in normal epidermis are Ca^{2+} independent and become Ca^{2+} dependent in response to wounding

To confirm and extend our previous observation that desmosomes in normal adult mouse epidermis are Ca^{2+} independent (Wallis et al., 2000), small pieces of epidermis (1 mm^3 or less) were dissected, placed in Ca^{2+}-free tissue-culture medium containing 3 mM ethylene glycol bis(2-aminoethyl ether)-N,N,N′N′-tetraacetic acid (EGTA), and incubated for up to 6 hours at 37°C. Controls were incubated in normal medium. They were then examined by electron microscopy. All desmosomes in normal epidermis remained intact after such treatment (Fig. 1A, Table 1) and were therefore Ca^{2+} independent.

Table 1. Calcium dependence of desmosomes in wounded and unwounded epidermis

	Unwounded	48 hours after wounding	72 hours after wounding
Number examined	200	400	400
Number Ca^{2+} dependent	0	221	255
% Ca^{2+} dependent	0	55.3	63.8

Pieces of unwounded epidermis and wound-edge epidermis 48 hours and 72 hours after wounding were harvested from four wounded mice at each time point and two unwounded mice. They were placed in LCM-EGTA for 6 hours and 2 hours, respectively, then fixed and examined by electron microscopy. One hundred desmosomes from each sample and, in the wounded cases, in cells up to 50 cell diameters from the wound edge were examined for calcium dependence.

To examine wound-edge epithelial desmosomes, similar experiments were carried out with fragments from a zone from the edges of full-thickness wounds on the backs of mice. A majority of desmosomes (55% by 48 hours and 63% by 72 hours) in wound-edge epithelium became Ca^{2+} dependent; adhesion was lost by separation of the desmosomal halves within 1 hour of exposure of wound-edge epidermis to EGTA (Fig. 1B, Table 1). This change was first detectable close to the wound edge (within 10 cell diameters) by 24 hours post wounding and spread throughout the entire wound-edge zone up to at least 50 cell diameters (~500 μm) by 48 hours. Thus desmosomes in wound-edge epidermis show similar changes to those previously reported in cultured sheets of MDCK cells (Wallis et al., 2000; Mattey and Garrod, 1986b).

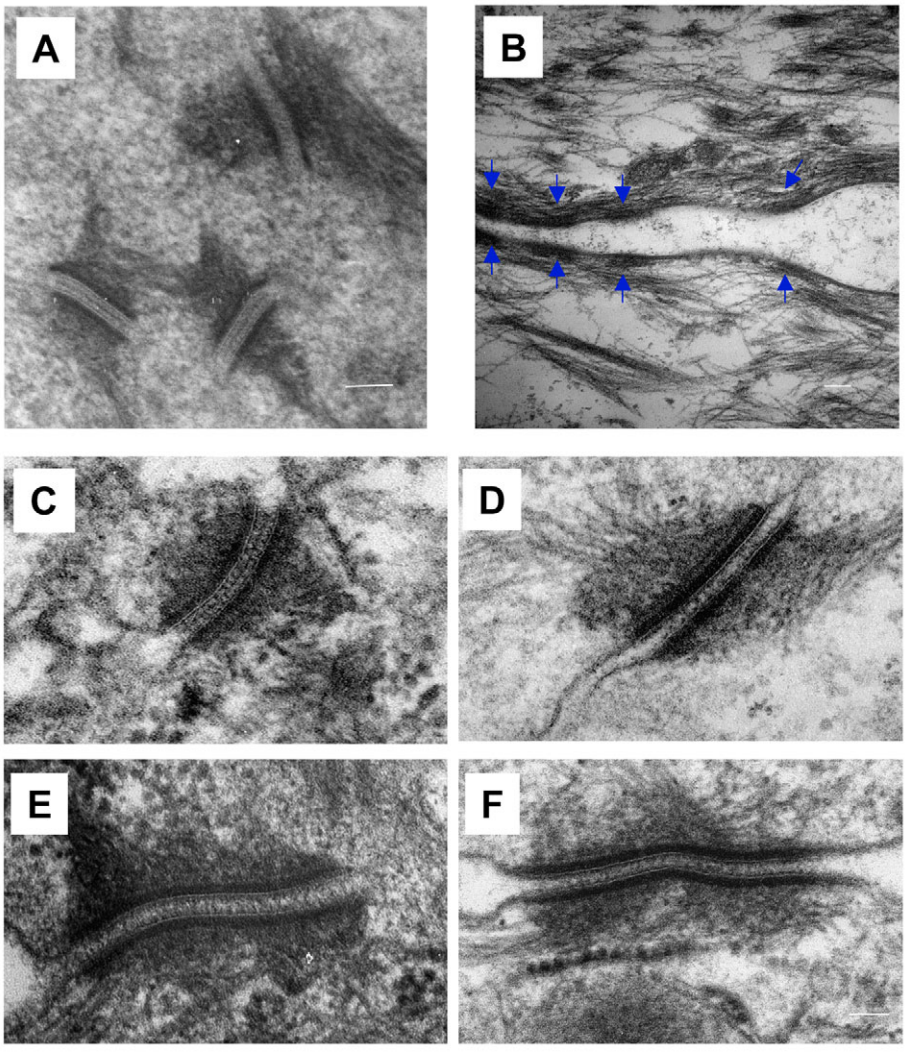

Fig. 1. Transmission electron micrographs of desmosomes in mouse epidermis. Normal (A) and wound-edge (B) mouse epidermis after exposure to calcium-free Dulbecco's minimum essential medium with 10% chelated foetal bovine serum and 3 mM EGTA (LCM-EGTA) for 6 hours (A) and 1 hour (B). Note that the desmosomes in A are intact and two that are sectioned precisely transversely exhibit midline structure, whereas in B the desmosomal halves (blue arrows) have lost adhesion and separated. Thus the desmosomes in A are calcium independent and those in B are calcium dependent. Quantification is shown in Table 1. (C-F) Comparison between desmosomes in unwounded and wound-edge epidermis. (C) Desmosome in unwounded epidermis showing characteristic midline structure. (D-F) Examples of transversely sectioned desmosomes from wound-edge epidermis showing absence of midlines. Quantification is shown in Table 2. Bars, 0.1 μm.

Table 2. Change of desmosome structure in wound epidermis

	Unwounded epidermis	Epidermis 48 hours after wounding
Number of animals	2	10
Number of desmosomes examined	200	1000
Number of desmosomes with changed structure	0	958

Desmosomes from four samples of intact epidermis and 20 wound edges showing change of desmosome structure, i.e. loss of midline, in transversely cut desmosomes of wound-edge epidermis, as determined by conventional transmission electron microscopy.

The desmosomal midline is lost and the intercellular space narrows in wound-edge epithelium

Change to Ca^{2+} dependence was associated with a remarkable change in desmosome structure (Fig. 1C-F; Table 2). Desmosomes in unwounded epidermis viewed in transverse section in electron micrographs possessed a dense midline joined to the plasma membrane by alternating cross-bridges on either side of the midline (Fig. 1A,C, Fig. 5A). By contrast, the majority of desmosomes in wound-edge epithelium showed no evidence of such dense structures (Fig. 1D-F). We also measured the width of the intercellular spaces of 50 desmosomes with and without midlines. Those with midlines were 23.9±0.5 nm in width and those without 21.9±0.5 nm (P=0.05 by Student's t-test). In addition we measured the width of the intercellular space of desmosomes from normal epidermis that had been exposed to 3 mM EGTA for 6 hours. These showed no significant difference from desmosomes exposed to normal culture medium for the same time. These desmosomes also retained the midline structure following EGTA exposure (Fig. 1A). We conclude that desmosomes in wound-edge epidermis show a spontaneous change in the organisation of their adhesive material compared with normal desmosomes. Furthermore, the adhesive material of normal, Ca^{2+}-independent desmosomes appears resistant to Ca^{2+} chelation.

PKCα becomes colocalised with the cytoplasmic plaques of desmosomes in wound-edge epithelium

We previously showed that PKCα became rapidly localised to the periphery of MDCK cells following wounding of confluent cultured cell sheets (Wallis et al., 2000). Furthermore, in unpublished observations, we showed that cell-peripheral PKCα was colocalised with desmosomal plaques. To determine whether similar changes take place in vivo, normal and wound-edge epidermis were examined by double-labelling immunofluorescence for PKCα and desmoplakin (a marker for desmosomes) with confocal microscopy, and by immuno-gold labelling of utra-thin cryosections.

PKCα was diffusely distributed in the cytoplasm principally of the basal cells of unwounded epidermis (Fig. 2A). On wounding, PKCα became colocalised with the desmosomal plaque, within 5 minutes at the extreme wound edge and by 48 hours 500 μm distant from the wound edge (Fig. 2A-F; Table 3A). Thus, in vivo as in culture, wounding epithelial cell sheets results in relocalisation of PKCα to desmosomal plaques.

We have previously mapped the locations of desmosomal component molecules within the desmosomal plaque by immuno-gold electron microscopy (North et al., 1999). To determine the distribution of PKCα in relation to other desmosomal plaque components, similar mapping was carried out using localisation of the C-terminus of desmoplakin with monoclonal antibody 11-5F as an internal control to check that no undue shrinkage had occurred and that our measurements were comparable with those we made previously (North et al., 1999).

Statistical analysis of the distribution of gold particles associated with anti-PKCα in the desmosomal plaque showed that they were not normally distributed because many particles were located very close to the plasma membrane. Rather, the analysis is consistent with the presence of a sharp peak of PKCα distribution ~1 nm from the inner face of the plasma membrane, and another, more diffuse peak centred around 23 nm, that is within the outer dense plaque (Fig. 2G,H; Table 3B). Comparison of this distribution with our map of the desmosomal plaque suggests that PKCα located very close to the plasma membrane may have the cytoplasmic domains of the desmosomal cadherins or plakophilin as its phosphorylation targets. PKCα located within the outer dense plaque may have a wider group of possible targets including the cadherin cytoplasmic domains, plakoglobin, plakophilin and the N-terminus of desmoplakin.

Table 3. Colocalisation of PKCα to desmosomes following wounding

A. Number of cells from wound edge showing colocalisation

Time after wounding	3-5 minutes	4 hours	8 hours	16 hours	24 hours	48 hours
Number of cells	2.9±0.1	4.3±0.1	5.7±0.1	12.8±0.3	18.1±0.3	50.0±0.0

B. Number of desmosomes labelled for immuno-gold PKCα in unwounded and wounded epidermis

	Unwounded epidermis	Within 20 cell diameters of wound edge	40-50 cell diameters from wound edge
% of desmosomes labelled for PKCα	0.03	97.1	88.5
Mean number of gold particles per desmosomal plaque	0.04	11.2	6.2

(A) Data from confocal immunofluorescence images showing spread of colocalisation of PKCα with desmoplakin with time after wounding. Numbers represent distance in terms of mean numbers of cells from the wound edge (±s.e.) in which colocalisation of PKCα with desmoplakin was detectable at different time points. Each time point represents 22 wound edges from 11 different animals. (B) Quantification of immuno-gold labelling of desmosomes in unwounded and wound-edge epidermis 72 hours after wounding from labelled ultra-thin cryosections. Each point represents analysis of 2000 desmosomes from 20 different wounds.

Desmosomes of wound-edge keratinocytes are internalised without splitting

To determine whether splitting of desmosomes occurred in wound-edge epithelium as part of the normal downregulatory process, the wound edge was examined by electron microscopy. By 48 hours after wounding all leading-wound-edge keratinocytes examined by electron microscopy showed substantial reduction in the numbers of desmosomes at their surfaces. No evidence for splitting of desmosomes as seen following EGTA treatment was found. Instead, 94 cells of 100 examined within ten cell diameters of the edges of 48-hour wounds showed whole intra-cytoplasmic desmosomes. Since 'cells' in this case means cell profiles seen in ultra-thin sections, it is probable that all cells in this region of the wound edge contained internalised desmosomes. Intra-cytoplasmic desmosomes were also occasionally noticed further from the

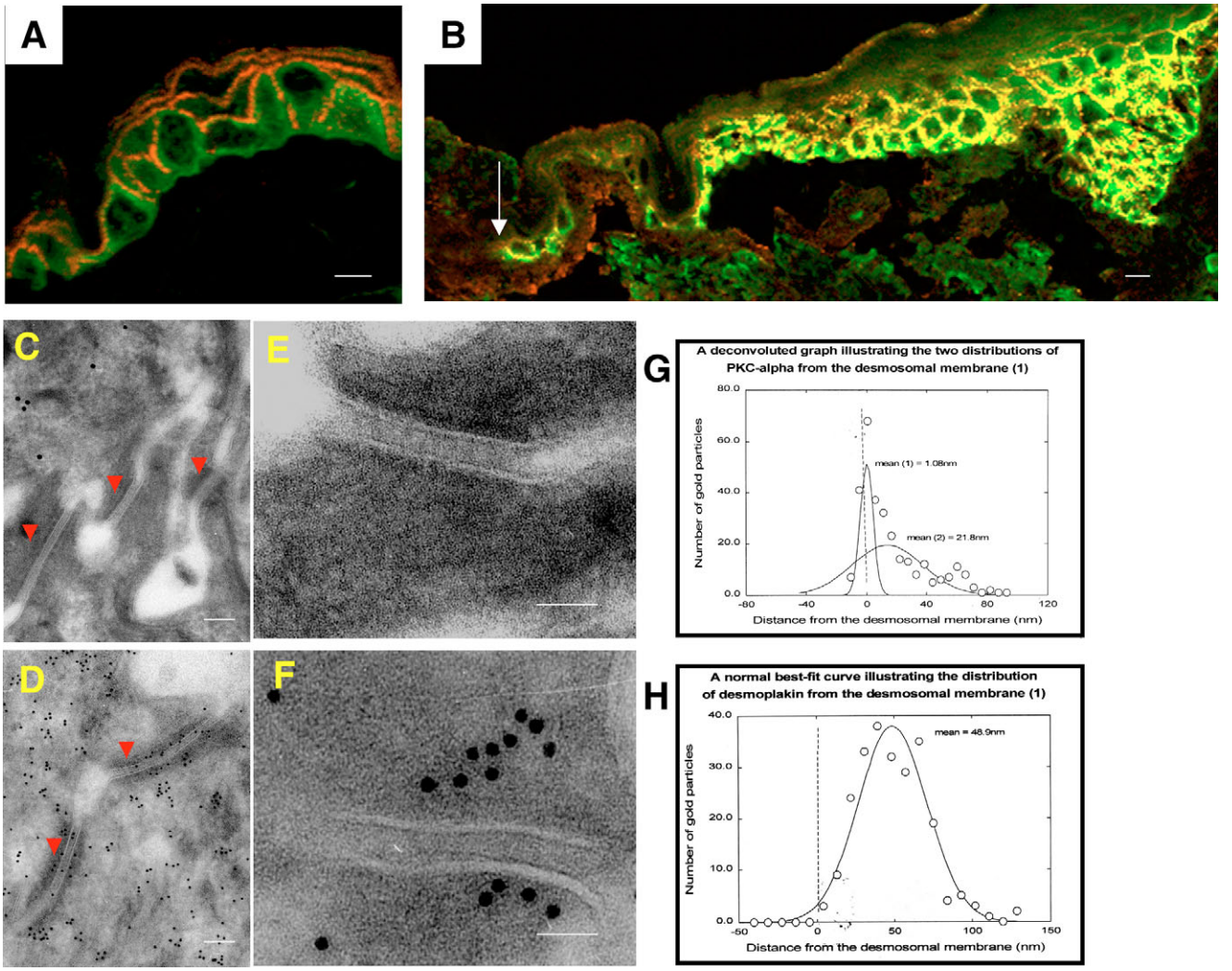

Fig. 2. PKCα is colocalised with desmoplakin in wound-edge epithelium after wounding. (A) In unwounded epidermis PKCα (green) is diffusely distributed in the cytoplasm of mouse keratinocytes and is not colocalised with desmoplakin (red). (B) By contrast, in wound-edge epithelium 72 hours post wounding, PKCα and desmoplakin show substantial colocalisation (yellow). The white arrow indicates the wound edge. Quantification of the spread of PKCα-desmoplakin colocalisation from the wound edge with time is shown in Table 3A. (C-F) Localisation of PKCα to desmosomal plaques by immuno-gold labelling of ultra-thin cryosections. Unwounded epidermis (C,E) and wound-edge epidermis (D, F) 48 hours after wounding. The desmosomes (red arrowheads in C and D) are unlabelled in normal epidermis, but the desmosomes and surrounding cytoplasm are heavily labelled in wound epidermis. Label in D that is not clearly associated with the two transversely sectioned desmosomes may be associated with desmosomal plaques cut en face or with intermediate filaments. Note none of the desmosomes show midlines because these structures are not visible by this technique (see North et al., 1999). Gold particles are 10 nm in diameter. Quantification of immuno-gold labelling in normal and 72 hour wound-edge epidermis is shown in Table 3B. (G,H) Distribution of PKCα in wound desmosomes. A low-resolution map of the desmosomal plaque from quantitative analysis of the distributions of gold particles after immuno-labelling with specific antibodies is published (North et al., 1999). To determine the distribution of PKCα in the desmosomal plaque, the distribution of PKCα labelling was similarly analysed in desmosomes that were double-labelled for desmoplakin C-terminus as an internal control. Particle distances from the cell membrane were determined. The peak of desmoplakin labelling was at 48.9 nm from the membrane (H), in good agreement with previous results (North et al., 1999). Deconvolution of the particle distribution suggested the presence of two PKCα peaks, one at 0.32-1.08 nm from the cell membrane and a much more diffuse peak at 18.2-21.8 nm from the membrane (G). The latter peak suggests localisation within the outer dense plaque of the desmosome (North et al., 1999). Bars, 5 μm (A,B); 0.1 μm (C,D); 30 nm (E,F).

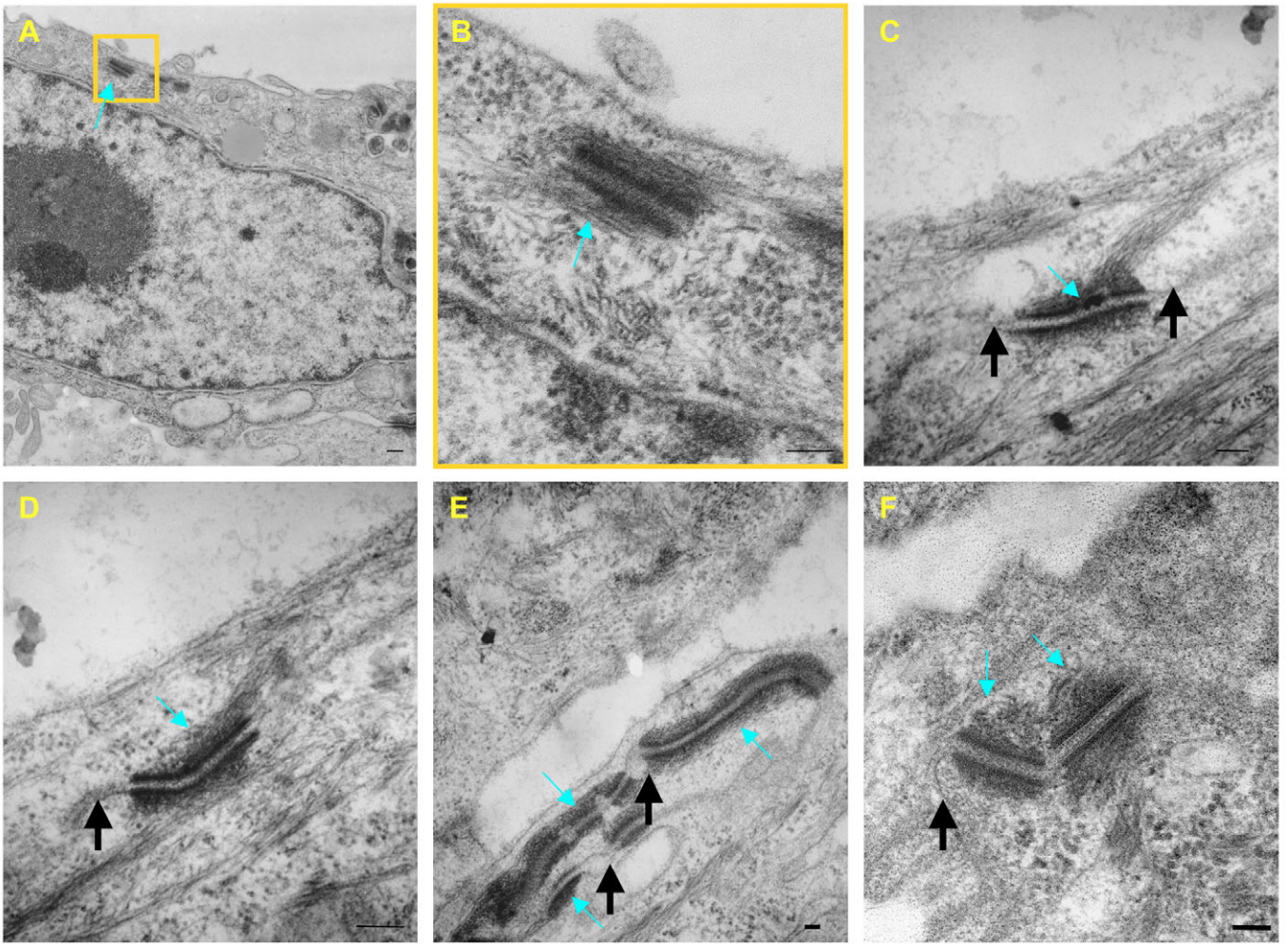

Fig. 3. Electron micrographs of intracytoplasmic desmosomes from mouse skin wounds. Images within 10 cell diameters (A-D) or 40-50 cell diameters from the wound edge (E,F), showing intracytoplasmic desmosomes (blue arrows). B is an enlargement of the area enclosed within the square in A. Note the absence of desmosomes from the cell surface membranes in all images. Black arrows indicate possible membrane fragments associated with some desmosomes. Bars, 100 nm.

edge; of 100 cells within the region of 40-50 cells from the edge examined in 48-hour wounds only 4 showed internalised desmosomes. Some internalised desmosomes appeared to be attached to membrane fragments (Fig. 3C-F), or to vesicles in the cytoplasm (not shown), giving the characteristic 'tennis-racket' shape reported by others (Caputo and Prandi, 1972). However, other internalised desmosomes appeared to have lost any associated membranous material, instead appearing free in the cytoplasm (Fig. 3B,F). We conclude that internalisation of entire desmosomes is the normal method of downregulation of desmosomal adhesion at the wound edge.

A model for the intercellular structure of Ca^{2+}-independent desmosomes

Several structural studies of classical cadherin fragments have shown that three Ca^{2+} ions bind at the linker regions between individual extracellular subdomains (Overduin et al., 1995; Shapiro et al., 1995). It is generally accepted that Ca^{2+} binding provides rigidity to the otherwise flexible linker region loops and accounts for the Ca^{2+} dependence of cadherin-mediated adhesion (Koch et al., 1997; Nagar et al., 1996; Pokutta et al., 1994). These studies indicate regular arrangements based on intramolecular and intermolecular interactions observed in the crystallographic cell, suggesting homophilic dimerisation of the cadherin extracellular domains in both cis (i.e. molecules on the same cell surface) and trans (i.e. molecules on opposite cell surfaces) (Boggon et al., 2002; Overduin et al., 1995; Shapiro et al., 1995). Trans interaction is clearly essential for adhesion and there is evidence to suggest that adhesion also requires cadherin clustering in cis (Brieher et al., 1996; Troyanovsky et al., 1999; Troyanovsky et al., 2003; Yap et al., 1997). Interestingly such regular structures, previously termed 'adhesion zippers', are more readily comparable to the ultrastructure of desmosomes than adherens junctions (Lasky, 1995).

Homology models for Dsc2 and Dsg2 were generated using the C-cadherin ectodomain as a template. Modelling of the desmosomal cadherins (Dsc2 and Dsg2) in the crystal packing observed for C-cadherin shows that it is feasible to produce a similar array, despite the modest sequence identity between them (~30%). However, some differences in detail between the intermolecular and intramolecular interactions in the

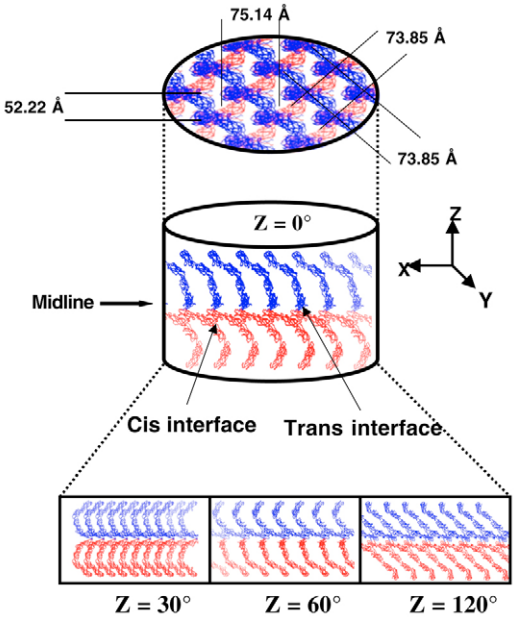

Fig. 4. Schematic representation of the Dsc2 ectodomain model 3D array, generated from the crystallographic structure of C-cadherin (Boggon et al., 2002). In the centre the desmosomal interspace is represented as a cylinder, showing the mid-line formed by trans and cis interactions between molecules on opposed cell surfaces. Monomers from one cell surface are coloured in red and monomers from the opposed cell surface are coloured in blue. The midline is aligned with the *x*-axis of the cylinder (coincident with the *x*-axis in the crystallographic lattice). Rotation of the 3D array around the *x*-axis by 90° (top) shows a regular lattice with distances between rows of molecules of 73.85 Å and distances of 75.14 Å between layers. Rotations around the *z*-axis produce four different views, all of them with a midline dense zone (bottom). These are: strand dimer 1 at z=0°; 'boat' at z=30°, strand dimer 2 (inverse form of strand dimer 1) at z=60° and 'zipper' at z=120°. The cis and trans interfaces between distal domains are indicated by arrows.

desmosomal cadherins maybe expected. The final quality of the models for Dsc2 and Dsg2 was compared with the C-cadherin structure. The root-mean-square deviation for all equivalent carbons was 1.03 Å for Dsc2 and 1.04 Å for Dsg2.

In an attempt to model the Ca^{2+}-independent desmosome structure we recreated a 3D array of Dsc2 molecules generated according to the crystallographic cell symmetry of C-cadherin. A similar array was generated for Dsg2. In these arrays, the adhesion interfaces are aligned to the *x*-axis (along the crystallographic *x*-axis) (Fig. 4 shows the Dsc2 array). In Fig. 4, the cylinder at the centre roughly represents the desmosomal interspace, containing the molecular stack. A front view (Z=0°) (Boggon et al., 2002), shows strand dimers formed in trans (trans interface) between monomers emanating from one cell surface (blue) and others emanating from the opposed cell surface (red). Rotation of the stack by 90° around the *x*-axis, shows a quadratic array (Fig. 4, top) with a repeating periodicity of 73.85 Å between rows of molecules, and a periodicity of 75.14 Å between layers. This array is remarkably similar to the en face view of the desmosome seen by lanthanum infiltration (Fig. 5), with a reported periodicity of 75 Å (Rayns et al., 1969). This quasi-crystalline arrangement was confirmed by digitisation and Fourier transformation of EM images (Rayns et al., 1969), revealing strong reflections characteristic of regularly ordered structures such as crystals (Fig. 5).

Rotation of the stack around the *z*-axis generates four different views: strand dimer 1 at z=0°, 'boat' view at z=30°, strand dimer 2 at z=60° and 'zipper' view at z=120° (Fig. 4, bottom). Each view occurs twice in a complete 360° rotation because of the crystallographic twofold symmetry axis aligned with the *x*-axis in Fig. 4. The 'zipper' view shows both cis and trans interactions. All four views show a concentration of material in the midline, which correlates well

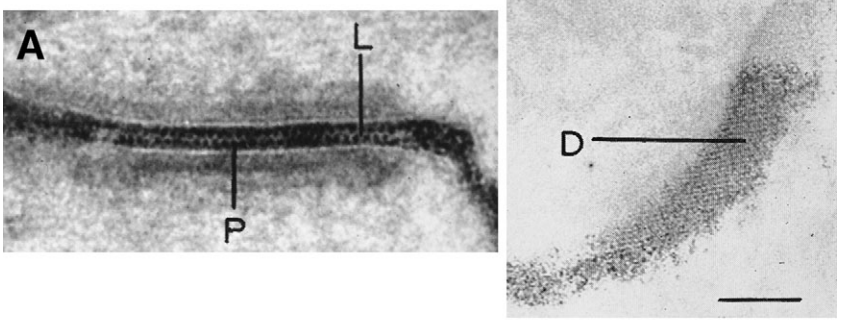

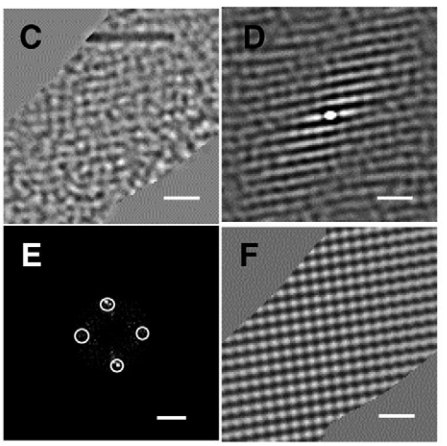

Fig. 5. (A) Transmission electron micrographs of a desmosome from guinea-pig heart after infiltration with lanthanum chloride cut in transverse section. Note how the mid line has a zigzag appearance. This arises because the dense particles (P) in one row are staggered with respect to those in the opposite row, and the pale central lamella (L) has side arms that extend between the particles. (B) En face view of lanthanum-infiltrated desmosome from guinea-pig heart showing a series of alternating dark and light parallel lines of 75 Å periodicity quadratic array of lanthanum-filled spaces. D, desmosome; J, gap junction. Images in A and B are reproduced from Rayns et al. (1969) by copyright permission of the Rockefeller University Press. (C) Extracted central region from image B after high-pass filtering and masking. (D) Autocorrelation image of C to show period structure. This shows both a strong lattice repeat of 75 Å and a second weaker lattice repeat of 72 Å with a direction about 85° to the first. (E) Power spectrum of image C with intensity peaks from the lattice structure circled. (F) Fourier-filtered image using a lattice mask based on the first order peaks shown in E. Bars, 0.1 μm (A,B); 200 Å (C,D,F); reciprocal space scale bar in E, 1/100 $Å^{-1}$.

with the midline observed by both conventional electron microscopy and freeze etching of desmosomes (Odland, 1958; Staehelin, 1974). Our comparative analysis of the 3D array for the Dsc2 model and the C-cadherin crystal with the EM data from desmosomes, shows evidence of a highly similar arrangement. Therefore, we propose that this 3D array is a good model for the highly ordered, quasi-crystalline desmosome structure observed in ultrastructural studies.

Ca^{2+}-independent desmosomes retain midline structure after prolonged exposure to EGTA (Fig. 1). Measurement of the intermembrane distance of 50 Ca^{2+}-independent desmosomes after treatment with 3 mM EGTA for 6 hours revealed no significant difference from controls, indicating that the structure is unaffected. Since both calcium-dependent desmosomes and adherens junctions (also calcium dependent) lack this highly ordered arrangement of the adhesive material, it may be that some feature of the regular array seen in the crystal structure makes an essential contribution to the Ca^{2+} independence of desmosomes. Trans interactions between cadherin molecules are clearly required for adhesion and must be present in both Ca^{2+}-dependent and Ca^{2+}-independent junctions. The key feature that distinguishes the crystallographic array is the cis-interaction interface involving binding of the EC1 domain from one molecule to the linker region between the EC2-EC3 domains in an adjacent molecule (Boggon et al., 2002). Therefore, these cis interactions may contribute to Ca^{2+} independence. We suggest that the cis interactions may result in the retention of calcium within the regular array according to the following argument.

The linker regions between the EC1 to EC5 subdomains domain of cadherins are involved in binding three Ca^{2+} ions at each interspace. Two of the ions (Ca1, Ca2) are buried in the main core of the protein domain with an octahedral coordination whereas the third Ca^{2+} ion (Ca3) is more exposed to the solvent. In the EC2-EC3 linker region Ca1 is coordinated by seven groups in N215, N217, D246, D248, A254 and N304 (C-cadherin numbering) and Ca3 by six ligands from residues E119, E182, D213, D216 and D248 (Fig. 6B). Ca3 is coordinated by four ligand groups in E119, D180, E182 and D216, where two side chains, from E119 and E182 are shared between Ca2 and Ca3. These Ca^{2+}-binding residues are fully conserved across all cadherins including the desmoglein and desmocollin. The different ligand coordination for the three positions correlates with marked differences in binding affinity for the three Ca^{2+} ions previously reported and with the notion that calcium binding restricts flexibility of the inter-domain region (Alattia et al., 1997; Koch et al., 1999; Koch et al., 1997; Pertz et al., 1999).

Analysis of the cis-interactions between EC1′ and EC2-EC3 (Fig. 6B) shows that the low-affinity Ca^{2+} ion (Ca3) is covered by the β-helix region of the EC1′ domain. This protection of the Ca3 binding site may limit its exchange with the solvent, and presumably its chelation by EGTA. According to this observation, we proposed the following model for the Ca^{2+}-independent hyper-adhesion in desmosomes. If, as we suggest, the extracellular domains of the desmosomal cadherins are able to form a quasi-crystalline array in which cis interactions are maximised, all of the Ca3 molecules at the EC2-EC3 boundaries would be protected and the structure of these interfaces would be maintained throughout upon exposure to EGTA. The regular array of cis interfaces would be matched by an equally regular array of trans interfaces, which are maintained by hydrophobic

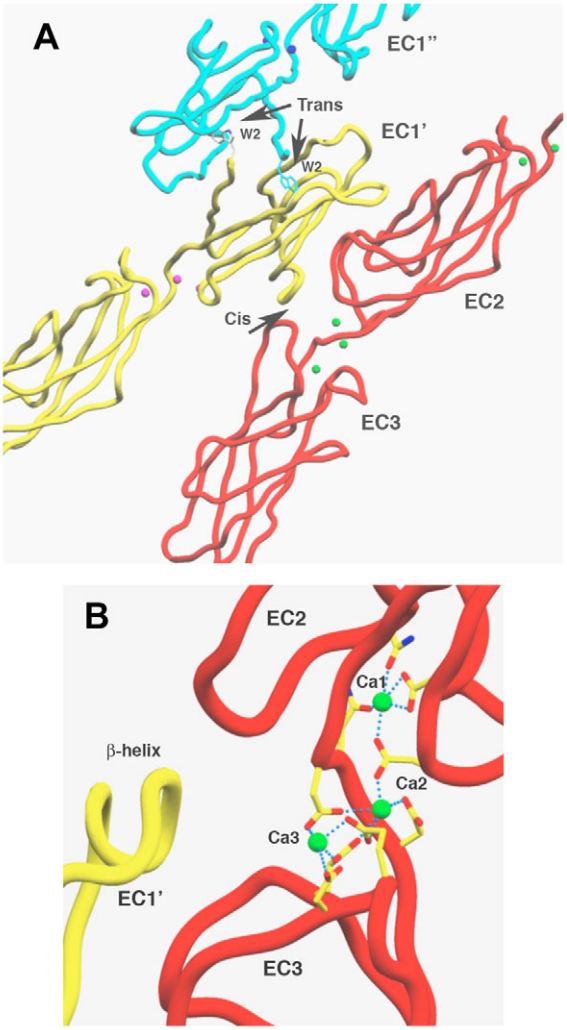

Fig. 6. (A) Detailed representation of the cis and trans interfaces in the 3D array packing generated with the Dsc2 model using the C-cadherin ectodomain structure (Boggon et al., 2002). Monomers from opposed cell surfaces (yellow and blue) form trans-interactions mediated by Trp2 in the N-terminal domain (EC1′ and EC1′′ respectively). The Trp side chain is shown binding into the hydrophobic pocket of the opposed N-terminal domain. Cis interactions occur between the EC1′ domain (yellow) and the linker region between the EC2 and EC3 domains on another monomer from the same cell surface (red). (B) Zoom view of the linker region. The EC1′ domain (yellow) from one monomer inserts the β-helix region, as a wedge, into the cavity formed between the EC2 and EC3 domains of a neighbouring molecule (red). This cis interface blocks access to the most-exposed calcium-binding site occupied by Ca3. The other two calcium ions, Ca1 and Ca2 are bound deeper into the core of domain EC2. Ca1 and Ca2 are coordinated by five ligand groups from different side chains and two groups from the main chain (not shown). Ca3 is coordinated only by four ligand groups from side chains in EC2 and EC3. The figure was prepared using SETOR.

interactions (Trp2 binding). The combined effect of these multiple interactions involving the EC1-EC3 subdomains would make possible a crystalline array structure that would provide strong, calcium-independent adhesion.

By contrast, in the calcium-dependent desmosome and the adherens junction, where the cadherin extracellular domains

are less ordered, we propose that the cis interactions would be either more dynamic or fewer in number. Addition of EGTA would then result in removal of some of the Ca3 ions, and a domino effect would result in collapse of all extracellular domains and loss of adhesion.

The calcium ions at the other EC subdomain interfaces have different coordination; Ca3 in EC3-EC4 has only two ligands and Ca3 at EC4-EC5 has six. The question arises as to whether they would be removed by exposure to EGTA. We envisage two possible scenarios. Either the ordered structure retains at least some of the calcium ions at these interfaces (certainly Ca1 and Ca2, which are strongly coordinated), or that the majority of the other calcium ions are removed, but the combined multiple interactions at the cis and trans interfaces in the mid line are sufficient to maintain adhesion.

Discussion

Hyper-adhesion: a unique and important property of desmosomes

Our results show that the vast majority of desmosomes in normal epidermis are Ca^{2+} independent. Previous results, although not quantitative, indicated that this was also true of desmosomes in several other tissues, including trachea, oesophagus, tongue, liver and cardiac muscle (Wallis et al., 2000). We suggest that Ca^{2+} independence is the normal state for desmosomes in adult tissues in vivo.

We refer to the Ca^{2+}-independent adhesive state of desmosomes as 'hyper-adhesion' because it appears to represent a higher-affinity, more stable state of adhesive binding than that shown by either Ca^{2+}-dependent desmosomes or other adhesive junctions such as adherens junctions. On wounding, when greater tissue lability is required to facilitate cell migration and wound repair, desmosomes spontaneously adopt a lower-affinity adhesive state. In doing so they appear to acquire characteristics that mimic those found in adherens junctions; they become Ca^{2+} dependent, their intercellular space narrows and they lose the highly organised structure of their adhesive material. A detailed consideration of the structure of adherens junctions is published elsewhere (Miyaguchi, 2000). Moreover, adherens junctions (and tight junctions) do not acquire Ca^{2+} independence (Wallis et al., 2000). Thus, we believe that hyper-adhesion represents a unique, more strongly adhesive state that can be adopted by desmosomes but not by other junctions. Furthermore we believe that hyper-adhesion can explain why desmosomes are so important in maintaining normal tissue architecture and function.

Clearly desmosomal hyper-adhesion is not the only reason for the strength of epithelial cell layers. Desmosomes and the intermediate filament cytoskeleton constitute a complex that forms a supporting scaffolding throughout an epithelium (Moll and Franke, 1982). When the intermediate filaments are disrupted, as in the human genetic disease epidermolysis bullosa and transgenic mice that mimic it, the epidermis is greatly weakened (Fuchs, 1996; Lane and McLean, 2004). Weakening or disrupting the interaction between desmosomes and intermediate filaments also diminishes the strength of epithelia (Huen et al., 2002; Russell et al., 2004). Scaffolding, like a chain, is only as strong as its weakest link. Thus desmosomal hyper-adhesion is crucial to the strength of the desmosome–intermediate-filament complex. We propose that the ability of desmosomes to adopt hyper-adhesiveness represents a specific evolutionary acquisition to enable them to fulfil their role in the complex.

The structure of Ca^{2+}-independent desmosomes

A remarkable feature of desmosomes that was revealed by early ultrastructural studies is the apparent highly ordered arrangement of the intercellular material, characteristically exemplified by an electron-dense midline half way between the opposed plasma membranes (Odland, 1958). We have shown that this structure is present when desmosomes are in their Ca^{2+}-independent, hyper-adhesive state, but absent from wound-edge epithelium when they become Ca^{2+} dependent and lose hyper-adhesiveness. This suggests that an organised structure of the adhesive material may be associated with high-affinity adhesion.

When this structure was infiltrated with the electron-dense tracer lanthanum, it appeared as a zigzag extending the full width of the junction and connected to the plasma membrane by alternating cross-bridges 30 Å in thickness (Rayns et al., 1969). In en face view, such infiltrates appeared as regular arrays of alternating white and black dotted lines with a periodicity of 75 Å. These observations suggest that the adhesive material of the desmosome has a quasi-crystalline arrangement. The crystal structures of the extracellular domains of classical cadherins, the adhesion molecules of adherens junctions, revealed such ordered structures that were referred to as 'adhesion zippers' and which bore striking resemblance to desmosomes (Lasky, 1995; Shapiro et al., 1995). In fact, as we showed, the spacings calculated from the crystallographic array are strikingly similar to those found in ultrastructural studies of desmosomes. We also built homology models for Dsc2 and Dsg2, which are fully compatible with the 3D array reported for C-cadherin. This evidence prompted us to consider this array as a good model for the hyper-adhesive desmosome. Obviously, the situation in vivo could differ from the observations in the crystal, mainly because the cytoplasmic regions of cadherins and associated proteins undoubtedly play an important role in assembly and organisation of the desmosome.

Such a crystalline array does not seem to comply with previous observations of adherens junctions, which even in their most elaborate form, show limited and discontinuous organisation of their adhesive material (Miyaguchi, 2000). We predict that in this case, the contribution of the cytoplasmic region may have a totally different effect on junction assembly and adhesiveness that compromises a highly ordered organisation. Unfortunately, structural data on the full-length cadherin are not yet available.

Our attempt to model the Ca^{2+}-independent desmosome from the crystal structure of C-cadherin produced two intriguing results. First, the periodicity shown in the en face views of the desmosome by electron microscopy and the C-cadherin crystal lattice are identical. Second, an arrangement of extracellular domains such as suggested by the C-cadherin lattice gives rise to a midline at no less than eight positions around the vertical axis. The appearance of the midline generated from such a structure might be expected to differ somewhat when viewed from different directions. It is not clear whether the preparation techniques used and the resolution achieved in conventional electron microscopy are adequate and sufficient to discriminate such differences.

A major consideration in modelling the desmosome was to attempt to seek an explanation for Ca^{2+}-independent adhesion by Ca^{2+}-dependent molecules. Our modelling was prompted by the consideration that Ca^{2+} independence seemed to be associated with ordered structure and Ca^{2+} dependence with lack of it. We show that Ca^{2+}-independent desmosomes retain midline structure after prolonged exposure to EGTA and measurement of the inter-membrane distance of Ca^{2+}-independent desmosomes after exposure to 3 mM EGTA for 6 hours revealed no significant difference from controls, indicating that the structure is unaffected. However, we do not know whether Ca^{2+} is removed from the desmosomes by such treatment, or is so tightly bound that it resists removal. Thus our model suggests that Ca^{2+} ions may be sequestered within the highly ordered, quasi-crystalline arrangement of the cadherin extracellular domains. The cis interactions between the molecules appear to be of key significance for this.

In the C-cadherin crystal structure the molecules are curved giving a predicted distance of 24.5 nm between the apposed plasma membranes of adhering cells (Boggon et al., 2002). This figure is very close to the intermembrane distance we measured for Ca^{2+}-independent desmosomes. A recent study has examined desmosome structure by cryo-electron microscopy of frozen sections following high-pressure rapid freezing of the tissue (Al-Amoudi et al., 2004). This showed a highly organised arrangement of the desmosomal cadherins, but showed them to be straight and indicated an inter-membrane distance of 34 nm. The structure shown by Al-Amoudi et al. (Al-Amoudi et al., 2004) is in fact remarkably similar to the predicted structure of a desmosome shown by Miyaguchi (Miyaguchi, 2000). It is not clear how cis interactions of the desmosomal cadherin extracellular domains would be accommodated in such a structure. The desmosomal interspace may appear somewhat shrunken by conventional transmission electron microscopy (Al-Amoudi et al., 2004), but its regularity of structure appears to be maintained.

We suggest that conversion to Ca^{2+} dependence involves a conformational rearrangement of the desmosomal cadherin extracellular domains. In the Ca^{2+}-dependent configuration they would be less organised and so would not give rise to the appearance of a midline. Adhesive binding would also be more easily disrupted. This may resemble the arrangement of classical cadherins in adherens junctions. A recent model of desmosome structure based on electron tomography of 2-day-old mouse epidermis suggested that the desmosomal cadherins have a disorganised, knotted arrangement in which cis interactions are compromised (He et al., 2003). We suggest that although trans interactions still occur in the Ca^{2+}-dependent state, fewer cis-dimerisation interactions may result in a gel-like structure similar to that proposed by He et al. (He et al., 2003), with higher plasticity than the more crystalline 3D mesh observed for Ca^{2+}-independent desmosomal structures. It may be that the desmosome chosen for analysis was Ca^{2+} dependent (He et al., 2003), but our unpublished observations show that the great majority of desmosomes in 2-day-old mouse epidermis are Ca^{2+} independent. We do not believe that the disorganised arrangement suggested (He et al., 2003) can account for the biological fact of Ca^{2+} independence.

A crucial component of this hypothesis is that the affinity of desmosomal adhesion is regulated by the phosphorylation of an

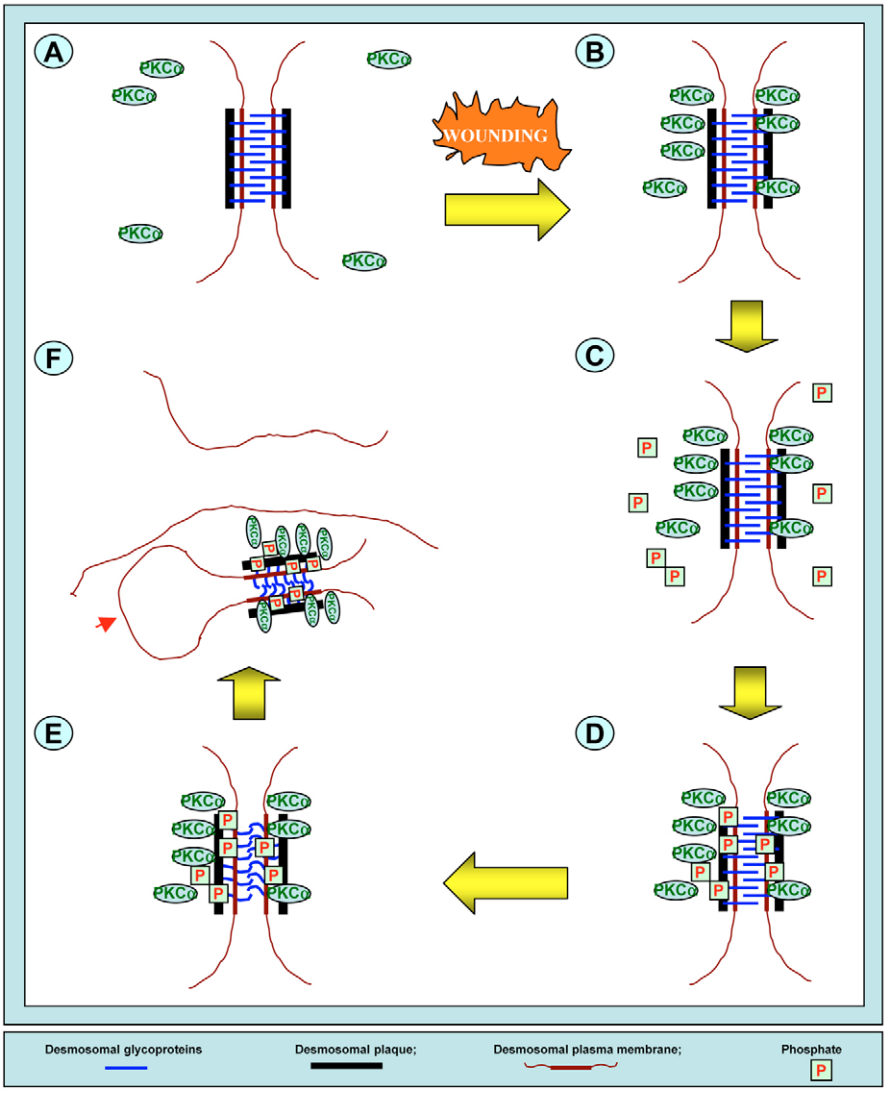

Fig. 7. Summary of events believed to lead to the downregulation of desmosomal adhesion in wounded epidermis. (A) In normal epidermis PKCα is diffusely distributed in keratinocyte cytoplasm, and desmosomes have an organised structure and are Ca^{2+} independent. (B) Following wounding PKCα associates with the desmosomal plaque. (C,D) PKCα mediates phosphorylation of desmosomal plaque component(s). (E) A transmembrane signal generates a less-organised arrangement of the desmosomal cadherins and onset of Ca^{2+} dependence. (F) Whole desmosomes are internalised by wound-edge cells probably initially in association with membrane vesicles (red arrow).

intracellular component(s) in the desmosomal plaque. We suggest that phosphorylation of one or more desmosomal components by PKCα may generate a transmembrane signal that alters the conformation of the extracellular domains of the desmosomal cadherins, reducing both their affinity for Ca^{2+} and their adhesive binding. This causes a relaxation in the extracellular domain so that the quasi-crystalline structure, exemplified by the midline, is lost. Although the midline disappears, adhesion is still maintained, for we have found no evidence for separation of desmosomal halves in wound-edge epithelium, except following the artificial exposure to EGTA. Recent evidence has shown that plakophilin 1, an armadillo-family protein and component of the desmosomal plaque, plays a role in regulating the Ca^{2+} independence of desmosomes (South et al., 2003). This supports our view that transmembrane effects are involved in regulating desmosomal adhesiveness.

It is well established for other adhesion molecules, especially integrins, that signals generated within the cytoplasm modulate the structure and binding affinity of the extracellular domains (Hynes et al., 2002; Liddington and Ginsberg, 2002). This is referred to as 'inside-out' signalling. We postulate that a cytoplasmic signal involving PKCα generates a similar inside-out signal in wound-edge epithelial cells, and that this modulates both the structure and binding affinity of desmosomal cadherins, converting them from Ca^{2+} independent to Ca^{2+} dependent.

Desmosomes in wound healing

Modulation or downregulation of desmosomes in wound-edge keratinocytes has been reported previously (Croft and Tarin, 1970). Our observations suggest that this downregulation is substantial and that it takes place by internalisation of whole desmosomes rather than by splitting into half desmosomes or by desmosome disassembly. To our knowledge this is a novel observation for wound-edge epithelium, although intracytoplasmic desmosomes have been reported in a variety of different skin lesions (Caputo and Prandi, 1972; Klingmuller et al., 1970; Klug and Haustein, 1974; Komura and Watanabe, 1975; Proctor and Sherman, 1975; Schenk, 1975; Schenk, 1980; Takaki et al., 1971; Watanabe et al., 1977) and in the trophoblast (Firth et al., 1980).

Internalisation of whole desmosomes was suggested as a mechanism for downregulation of desmosomes in the epidermis (Allen and Potten, 1975). The desmosomes appeared to be engulfed in a double-membrane vesicle derived from the two adjacent cells that had formed the desmosomes. Some of the internalised desmosomes that we have observed at the wound edge had membrane associated with them, but others seemed to have no membrane. We have no explanation for this apparently common occurrence.

Our suggestion and summary of the sequence of events that accompanies desmosomal downregulation is shown in Fig. 7. What is the role of PKCα in this event? We note that PKC signalling has been shown to be associated with endocytosis and phagocytosis in a number of different systems (Hirai, 2001; Lennartz, 1999; Liu and Anand, 2001; Scaife and Margolis, 1997; Wright et al., 1997) and therefore suggest that PKC signalling in some way primes desmosomes for internalisation by a process akin to phagocytosis. Thus primed, the desmosomes remain weakly adhesive in the wound-edge epithelium until a further signal associated with the onset of cell motility promotes their internalisation. Work in our laboratory currently aims to discover the mechanism of this process. Most importantly, our work has shown how desmosomes ensure a stable network of cells in a physically stressed environment.

We thank the Medical Research Council for financial support and the Egyptian Government for support to M.Y.B. We also thank Jordi Bella, Anita Merritt, Martin Humphries, Charles Streuli, Zhuxiang Nie, Nigel Hodson, Gillian Ashcroft and Diane Silla for valuable help and discussions during the preparation of the manuscript.

References

Al-Amoudi, A., Norlen, L. P. and Dubochet, J. (2004). Cryo-electron microscopy of vitreous sections of native biological cells and tissues. *J. Struct. Biol.* **148**, 131-135.

Alattia, J. R., Ames, J. B., Porumb, T., Tong, K. I., Heng, Y. M., Ottensmeyer, P., Kay, C. M. and Ikura, M. (1997). Lateral self-assembly of E-cadherin directed by cooperative calcium binding. *FEBS Lett.* **417**, 405-408.

Allen, T. D. and Potten, C. S. (1975). Desmosomal form, fate, and function in mammalian epidermis. *J. Ultrastruct. Res.* **51**, 94-105.

Boggon, T. J., Murray, J., Chappuis-Flament, S., Wong, E., Gumbiner, B. M. and Shapiro, L. (2002). C-cadherin ectodomain structure and implications for cell adhesion mechanisms. *Science* **296**, 1308-1313.

Borysenko, J. Z. and Revel, J. P. (1973). Experimental manipulation of desmosome structure. *Am. J. Anat.* **137**, 403-421.

Brieher, W. M., Yap, A. S. and Gumbiner, B. M. (1996). Lateral dimerization is required for the homophilic binding activity of C-cadherin. *J. Cell Biol.* **135**, 487-496.

Brunger, A. T., Kuriyan, J. and Karplus, M. (1987). Crystallographic R factor refinement by molecular dynamics. *Science* **235**, 458-460.

Caputo, R. and Prandi, G. (1972). Intracytoplasmic desmosomes. *J. Ultrastruct. Res.* **41**, 358-368.

Chidgey, M. (2002). Desmosomes and disease: an update. *Histol. Histopathol.* **17**, 1179-1192.

Croft, C. B. and Tarin, D. (1970). Ultrastructural studies of wound healing in mouse skin. I. Epithelial behaviour. *J. Anat.* **106**, 63-77.

Firth, J. A., Farr, A. and Bauman, K. (1980). The role of gap junctions in trophoblastic cell fusion in the guinea-pig placenta. *Cell Tissue Res.* **205**, 311-318.

Fuchs, E. (1996). The cytoskeleton and disease: genetic disorders of intermediate filaments. *Annu. Rev. Genet.* **30**, 197-231.

Garrod, D. R., Merritt, A. J. and Nie, Z. (2002a). Desmosomal adhesion: structural basis, molecular mechanism and regulation (Review). *Mol. Membr. Biol.* **19**, 81-94.

Garrod, D. R., Merritt, A. J. and Nie, Z. (2002b). Desmosomal cadherins. *Curr. Opin. Cell. Biol.* **14**, 537-545.

Getsios, S., Huen, A. C. and Green, K. J. (2004). Working out the strength and flexibility of desmosomes. *Nat. Rev. Mol. Cell. Biol.* **5**, 271-281.

Haussinger, D., Ahrens, T., Aberle, T., Engel, J., Stetefeld, J. and Grzesiek, S. (2004). Proteolytic E-cadherin activation followed by solution NMR and X-ray crystallography. *EMBO J.* **23**, 1699-1708.

He, W., Cowin, P. and Stokes, D. L. (2003). Untangling desmosomal knots with electron tomography. *Science* **302**, 109-113.

Hennings, H. and Holbrook, K. A. (1983). Calcium regulation of cell-cell contact and differentiation of epidermal cells in culture. An ultrastructural study. *Exp. Cell. Res.* **143**, 127-142.

Hirai, H. (2001). Modification of AMPA receptor clustering regulates cerebellar synaptic plasticity. *Neurosci. Res.* **39**, 261-267.

Huber, O. (2003). Structure and function of desmosomal proteins and their role in development and disease. *Cell. Mol. Life. Sci.* **60**, 1872-1890.

Huen, A. C., Park, J. K., Godsel, L. M., Chen, X., Bannon, L. J., Amargo, E. V., Hudson, T. Y., Mongiu, A. K., Leigh, I. M., Kelsell, D. P. et al. (2002). Intermediate filament-membrane attachments function synergistically with actin-dependent contacts to regulate intercellular adhesive strength. *J. Cell Biol.* **159**, 1005-1017.

Hynes, R. O., Lively, J. C., McCarty, J. H., Taverna, D., Francis, S. E., Hodivala-Dilke, K. and Xiao, Q. (2002). The diverse roles of integrins and

their ligands in angiogenesis. *Cold Spring Harb. Symp. Quant. Biol.* **67**, 143-153.

Kartenbeck, J., Schmid, E., Franke, W. W. and Geiger, B. (1982). Different modes of internalization of proteins associated with adherens junctions and desmosomes: experimental separation of lateral contacts induces endocytosis of desmosomal plaque material. *EMBO J.* **1**, 725-732.

Klingmuller, G., Klehr, H. U. and Ishibashi, Y. (1970). Desmosomes in the cytoplasm of dedifferentiated keratinocytes of squamous cell carcinoma. *Arch. Klin. Exp. Dermatol.* **238**, 356-365.

Klug, H. and Haustein, U. F. (1974). Occurrence of intracytoplasmic desmosomes in keratinocytes (author's transl.). *Dermatologica* **148**, 143-153.

Koch, A. W., Pokutta, S., Lustig, A. and Engel, J. (1997). Calcium binding and homoassociation of E-cadherin domains. *Biochemistry* **36**, 7697-7705.

Koch, A. W., Bozic, D., Pertz, O. and Engel, J. (1999). Homophilic adhesion by cadherins. *Curr. Opin. Struct. Biol.* **9**, 275-281.

Komura, J. and Watanabe, S. (1975). Desmosome-like structures in the cytoplasm of normal human keratinocyte. *Arch. Dermatol. Res*. **253**, 145-149.

Lane, E. B. and McLean, W. H. (2004). Keratins and skin disorders. *J. Pathol.* **204**, 355-366.

Lasky, L. A. (1995). From sticky zippers to morphology. *Nat. Struct. Biol.* **2**, 258-261.

Lennartz, M. R. (1999). Phospholipases and phagocytosis: the role of phospholipid-derived second messengers in phagocytosis. *Int. J. Biochem. Cell Biol.* **31**, 415-430.

Levitt, M. (1992). Accurate modeling of protein conformation by automatic segment matching. *J. Mol. Biol.* **226**, 507-533.

Liddington, R. C. and Ginsberg, M. H. (2002). Integrin activation takes shape. *J. Cell Biol.* **158**, 833-839.

Liu, J. G. and Anand, K. J. (2001). Protein kinases modulate the cellular adaptations associated with opioid tolerance and dependence. *Brain Res. Brain Res. Rev.* **38**, 1-19.

Mattey, D. L. and Garrod, D. R. (1986a). Calcium-induced desmosome formation in cultured kidney epithelial cells. *J. Cell Sci.* **85**, 95-111.

Mattey, D. L. and Garrod, D. R. (1986b). Splitting and internalization of the desmosomes of cultured kidney epithelial cells by reduction in calcium concentration. *J. Cell Sci.* **85**, 113-124.

McMillan, J. R. and Shimizu, H. (2001). Desmosomes: structure and function in normal and diseased epidermis. *J. Dermatol.* **28**, 291-298.

Miyaguchi, K. (2000). Ultrastructure of the zonula adherens revealed by rapid-freeze deep-etching. *J. Struct. Biol.* **132**, 169-178.

Moll, R. and Franke, W. W. (1982). Intermediate filaments and their interaction with membranes. The desmosome-cytokeratin filament complex and epithelial differentiation. *Pathol. Res. Pract.* **175**, 146-161.

Nagar, B., Overduin, M., Ikura, M. and Rini, J. M. (1996). Structural basis of calcium-induced E-cadherin rigidification and dimerization. *Nature* **380**, 360-364.

Nollet, F., Kools, P. and van Roy, F. (2000). Phylogenetic analysis of the cadherin superfamily allows identification of six major subfamilies besides several solitary members. *J. Mol. Biol.* **299**, 551-572.

North, A. J., Bardsley, W. G., Hyam, J., Bornslaeger, E. A., Cordingley, H. C., Trinnaman, B., Hatzfeld, M., Green, K. J., Magee, A. I. and Garrod, D. R. (1999). Molecular map of the desmosomal plaque. *J. Cell Sci*. **112**, 4325-4336.

Odland, G. F. (1958). The fine structure of the interrelationship of cells in the human epidermis. *J. Biophys. Biochem. Cytol.* **4**, 529-538.

Overduin, M., Harvey, T. S., Bagby, S., Tong, K. I., Yau, P., Takeichi, M. and Ikura, M. (1995). Solution structure of the epithelial cadherin domain responsible for selective cell adhesion. *Science* **267**, 386-389.

Parrish, E. P., Steart, P. V., Garrod, D. R. and Weller, R. O. (1987). Antidesmosomal monoclonal antibody in the diagnosis of intracranial tumours. *J. Pathol*. **153**, 265-273.

Payne, A. S., Hanakawa, Y., Amagai, M. and Stanley, J. R. (2004). Desmosomes and disease: pemphigus and bullous impetigo. *Curr. Opin. Cell Biol.* **16**, 536-543.

Pertz, O., Bozic, D., Koch, A. W., Fauser, C., Brancaccio, A. and Engel, J. (1999). A new crystal structure, Ca2+ dependence and mutational analysis reveal molecular details of E-cadherin homoassociation. *EMBO J.* **18**, 1738-1747.

Pokutta, S., Herrenknecht, K., Kemler, R. and Engel, J. (1994). Conformational changes of the recombinant extracellular domain of E-cadherin upon calcium binding. *Eur. J. Biochem.* **223**, 1019-1026.

Proctor, S. J. and Sherman, K. C. (1975). Ultrastructural changes in bovine lingual epithelium infected with vesicular stomatitis virus. *Vet. Pathol.* **12**, 362-377.

Rayns, D. G., Simpson, F. O. and Ledingham, J. M. (1969). Ultrastructure of desmosomes in mammalian intercalated disc; appearances after lanthanum treatment. *J. Cell Biol.* **42**, 322-326.

Runswick, S. K., O'Hare, M. J., Jones, L., Streuli, C. H. and Garrod, D. R. (2001). Desmosomal adhesion regulates epithelial morphogenesis and cell positioning. *Nat. Cell Biol.* **3**, 823-830.

Russell, D., Andrews, P. D., James, J. and Lane, E. B. (2004). Mechanical stress induces profound remodelling of keratin filaments and cell junctions in epidermolysis bullosa simplex keratinocytes. *J. Cell Sci.* **117**, 5233-5243.

Scaife, R. M. and Margolis, R. L. (1997). The role of the PH domain and SH3 binding domains in dynamin function. *Cell Signal.* **9**, 395-401.

Schenk, P. (1975). Desmosomal structures in the cytoplasm of normal and abnormal keratinocytes (author's transl). *Arch. Dermatol. Res.* **253**, 23-42.

Schenk, P. (1980). Intracytoplasmic desmosomes in malignant keratinocytes of laryngeal carcinoma. *Arch. Otorhinolaryngol.* **226**, 219-223.

Shapiro, L., Fannon, A. M., Kwong, P. D., Thompson, A., Lehmann, M. S., Grubel, G., Legrand, J. F., Als-Nielsen, J., Colman, D. R. and Hendrickson, W. A. (1995). Structural basis of cell-cell adhesion by cadherins. *Nature* **374**, 327-337.

Skerrow, C. J., Clelland, D. G. and Skerrow, D. (1989). Changes to desmosomal antigens and lectin-binding sites during differentiation in normal human epidermis: a quantitative ultrastructural study. *J. Cell Sci.* **92**, 667-677.

South, A. P. (2004). Plakophilin **1**, an important stabilizer of desmosomes. *Clin. Exp. Dermatol.* **29**, 161-167.

South, A. P., Wan, H., Stone, M. G., Dopping-Hepenstal, P. J., Purkis, P. E., Marshall, J. F., Leigh, I. M., Eady, R. A., Hart, I. R. and McGrath, J. A. (2003). Lack of plakophilin 1 increases keratinocyte migration and reduces desmosome stability. *J. Cell Sci.* **116**, 3303-3314.

Staehelin, L. A. (1974). Structure and function of intercellular junctions. *Int. Rev. Cytol.* **39**, 191-283.

Takaki, Y., Masutani, M. and Kawada, A. (1971). Electron microscopic study of keratoacanthoma. *Acta Derm. Venereol.* **51**, 21-26.

Tomlinson, A. and Ferguson, M. W. (2003). Wound healing: a model of dermal wound repair. *Methods. Mol. Biol.* **225**, 249-260.

Troyanovsky, R. B., Klingelhofer, J. and Troyanovsky, S. (1999). Removal of calcium ions triggers a novel type of intercadherin interaction. *J. Cell. Sci.* **112**, 4379-4387.

Troyanovsky, R. B., Sokolov, E. and Troyanovsky, S. M. (2003). Adhesive and lateral E-cadherin dimers are mediated by the same interface. *Mol. Cell. Biol.* **23**, 7965-7972.

Tselepis, C., Chidgey, M., North, A. and Garrod, D. (1998). Desmosomal adhesion inhibits invasive behavior. *Proc. Natl. Acad. Sci. USA* **95**, 8064-8069.

Vasioukhin, V., Bauer, C., Yin, M. and Fuchs, E. (2000). Directed actin polymerization is the driving force for epithelial cell-cell adhesion. *Cell* **100**, 209-219.

Vasioukhin, V., Bowers, E., Bauer, C., Degenstein, L. and Fuchs, E. (2001). Desmoplakin is essential in epidermal sheet formation. *Nat. Cell Biol.* **3**, 1076-1085.

Wallis, S., Lloyd, S., Wise, I., Ireland, G., Fleming, T. P. and Garrod, D. (2000). The alpha isoform of protein kinase C is involved in signaling the response of desmosomes to wounding in cultured epithelial cells. *Mol. Biol. Cell* **11**, 1077-1092.

Watanabe, S., Komura, J. and Ofuji, S. (1977). Ultrastructural studies of epidermal lesions in pityriasis lichenoides chronica: occurrence of tubular aggregates and intracytoplasmic desmosomes. *Br. J. Dermatol*. **96**, 59-66.

Watt, F. M., Mattey, D. L. and Garrod, D. R. (1984). Calcium-induced reorganization of desmosomal components in cultured human keratinocytes. *J. Cell Biol*. **99**, 2211-2215.

Wright, E. M., Hirsch, J. R., Loo, D. D. and Zampighi, G. A. (1997). Regulation of Na+/glucose cotransporters. *J. Exp. Biol.* **200**, 287-293.

Yap, A. S., Brieher, W. M., Pruschy, M. and Gumbiner, B. M. (1997). Lateral clustering of the adhesive ectodomain: a fundamental determinant of cadherin function. *Curr. Biol*. **7**, 308-315.